

A study of field performance and sustainability of Fluoride Nilogon in defluoridation in Yemen

Tushmita Das^a, Saranga Baishya^a, Priya Devi^a, Anwesha Chaliha^a, Amal Hasan^b, Sara Bazarah^b, Wasim Al Shehab^b, Radwan Mohammed Saleh^b, Hammam Mukred^b, Mohammed Riyadh^b, Akram Al-Melhani^b, Gerrienne Pennings^b, Bereket Godifay Kahsay^b, Matthijs T. Wessels^c, Harm Bouta^c, Robin K. Dutta^{a,*}

^a Department of Chemical Sciences, Tezpur University, Napaam, Assam 784028, India

^b ZOA, 856X+WFX, 15 St, Haddah, Sana'a, Yemen

^c ZOA, Sleutebloemstraat 45, PO Box 4130, Apeldoorn 7320 AC, the Netherlands

ARTICLE INFO

Keywords:

Fluoride removal
Suitability of limestone
Field performance
Fluoride in Yemen

ABSTRACT

Yemen faces a severe drinking water crisis due to rapidly declining groundwater and elevated fluoride concentrations exceeding WHO guidelines. In areas with fluoride contamination, such as Lahj and Al Dhale'a governorates, where groundwater is the only drinking water source available, the risks to public health are high. To address this, ZOA, an international relief and recovery organisation, in collaboration with Tezpur University, piloted the low-cost Fluoride Nilogon filter, developed by a Tezpur University group, across 300 households in Lahj governorate as Phase I in 2021. Based on its demonstrated effectiveness, the intervention was expanded in Phase II to 400 additional households in Al Dhale'a and a communal scale unit (18,000 L size) treating ~7000 L per batch, benefitting approximately 700 residents in Al Dhale'a governorate in 2024. This paper describes a study of the field performance of the filters in both phases, offering a scalable solution for decentralised fluoride alleviation in low-resource environments. The paper also includes a study of suitability of the crushed limestone for Fluoride Nilogon reactors for both phases of the intervention and the performance of the filters. The suitability of limestone for field use was analysed by obtaining four samples of limestone, viz., A and B in Phase I; and C and D in Phase II, obtained from various localities of Yemen, to choose the better one for field use. The results of the fluoride removal abilities of the limestone samples were correlated with major physicochemical characteristics of limestone, such as porosity, density, and chemical impurities.

1. Introduction

Groundwater constitutes a vital renewable natural resource integral to the hydrological cycle. Concomitant with population growth, dependence on groundwater is increasing exponentially, particularly in developing nations where it represents the primary source of potable water (Costantini et al., 2023; Xu et al., 2021). Over 2.5 billion individuals rely on groundwater for safe drinking water, out of which, more than 0.5 billion across 106 countries are affected by groundwater quality issues, including fluoride contamination (Shaji et al., 2021). Fluoride, a prevalent anion in groundwater worldwide, is essential for dental health when present in the optimal concentration of 0.5–1.0 mgL⁻¹, which also helps prevent tooth decay. However, it

possesses a significant challenge to the provision of safe drinking water when present in excess concentration with potential adverse health effect such as skeletal and dental fluorosis (Susheela, 2007). The World Health Organization (WHO) has prescribed an upper guideline value of 1.5 mgL⁻¹ for fluoride in drinking water (WHO, 2017). Instances of elevated fluoride concentrations exceeding its guideline value have been documented in numerous countries across Americas, Africa, and Asia including the Middle East, rendering groundwater unsuitable for human consumption (Ahmad et al., 2022; Amini et al., 2008; Shaji et al., 2024).

Access to safe drinking water remains tragically out of reach for millions in conflict-ridden regions. Yemen, situated in a semi-arid to arid zone, already faced significant water scarcity challenges. The ongoing conflict has precipitated a catastrophic humanitarian crisis, with access

* Corresponding author.

E-mail address: robind@tezu.ernet.in (R.K. Dutta).

<https://doi.org/10.1016/j.clwat.2025.100160>

Received 12 September 2025; Received in revised form 16 October 2025; Accepted 25 October 2025

Available online 28 October 2025

2950-2632/© 2025 The Author(s). Published by Elsevier Ltd. This is an open access article under the CC BY license (<http://creativecommons.org/licenses/by/4.0/>).

to safe drinking water drastically curtailed, and exacerbating existing vulnerabilities. In this context, access to safe drinking water is not just a challenge, but also a desperate struggle for survival, further compounding the already dire humanitarian situation in Yemen (UNICEF, 2025; Varisco, 2019; Weiss, 2015). Furthermore, many groundwater sources in Yemen contain fluoride concentrations above WHO guidelines, posing an additional health risk (Aqeel et al., 2017; Al-Hmani et al., 2024). In Yemen, bone disease and dental fluorosis are observed in many areas because of the excessive intake of fluoride (Baghel, 2015). Reports from the government indicate high fluoride content in groundwater in governorates such as Sana'a, Ibb, Dhamar, Taiz, Lahj, Al Dhale'a and Raimah, with concentrations far exceeding the guideline value prescribed by WHO (Al-Amry et al., 2020). While both the government and the Yemen WASH (Water, Sanitation and Hygiene) sector acknowledge the presence and risk of fluoride in drinking water, hardly any cost-effective interventions to reduce fluoride levels have taken place so far. This is mainly due to the lack of low-cost treatment options and the nature of short-term humanitarian interventions that focus on access and quantity of water supply rather than on quality.

While providing fluoride-free surface water is the ideal solution to this problem, delivering this water via pipelines to remote and sparsely populated rural areas may be impractical due to logistical and economic constraints. Several defluoridation techniques based on adsorption, ion-exchange, precipitation, reverse osmosis, electrocoagulation, photocatalysis, membrane filtration and electrodialysis have been developed in the recent time (Arab et al., 2024; Gogoi and Dutta, 2016; Gourai et al., 2023; Nath and Dutta, 2010; Pan et al., 2019; Rath et al., 2024).

Selection of an appropriate defluoridation method remains a complex task, in humanitarian crisis settings like Yemen, where high fluoride concentration in groundwater demands a solution that is simultaneously highly efficient, cost-effective, and low energy. Conventional approaches such as adsorption are generally more cost-effective and simpler to implement but they are often limited by lower lifespan and require timely regeneration. Advanced technologies like membrane filtration and electrocoagulation offer superior performance but at the expense of higher operational costs (Crini and Lichtfouse, 2019). Reverse osmosis (RO) and electrodialysis, are constrained by their high energy demand and high capital cost making them unsuitable for remote, decentralized community use especially for treating water with high fluoride concentrations. A huge quantity of reject water is also another disadvantage of RO. Thus, there is a need for a robust, simple, and locally deployable technology that can achieve compliance with WHO standards without relying on a consistent power supply.

The phosphoric acid-crushed limestone treatment (PACLT) method, popularly known as Fluoride Nilogon, is an effective hybrid adsorption and precipitation-based technology that has been increasingly implemented in several fluoride-affected regions of India with high fluoride levels (up to 20mgL^{-1}), including Assam, Chhattisgarh, Odisha, Karnataka, and Rajasthan (Gogoi et al., 2015; Gupta et al., 2021; Mohan et al., 2020). The method was developed by a research group at Tezpur University in Assam, India and was implemented in some rural areas of Assam in the beginning, and so the Assamese word, Nilogon for removal, came in the name. Several studies have affirmed the environmental and economic sustainability of this approach, emphasizing its operational simplicity, minimal maintenance requirements, low implementation costs, and the notable advantage of functioning without the need for electricity (Das et al., 2025; Gogoi and Dutta, 2016; Gogoi et al., 2015; Gupta et al., 2021; Mohan and Dutta 2020b, 2020a; Nath and Dutta, 2010). However, the efficiency of fluoride removal using the PACLT method is significantly influenced by various operational parameters, including the particle size of the crushed limestone, contact time, pH control, and the stoichiometric ratio between phosphoric acid and limestone. Furthermore, the quality parameters of the limestone, such as density, porosity, hardness, and presence of iron and aluminium impurities, determine suitability of the limestone for Fluoride Nilogon, though almost 60 % of the limestone samples from different mines or

sources across India and the rift valley of Africa have been reported to be suitable (Mohan and Dutta, 2020a). Recent studies have demonstrated its potential for the simultaneous removal of other pollutants, such as hexavalent chromium, thereby extending the applicability of PACLT beyond fluoride mitigation (Das et al., 2025).

ZOA ('Zuidoost Azië', Dutch words for 'Southern Asia'), an international relief and recovery organization, has been actively involved in addressing the drinking water crisis in Yemen since 2012. Given the remote nature of the locations of Yemen, where ZOA encountered water sources with high fluoride levels, low-tech and low-cost options have been preferred to assess. In 2021, ZOA collaborated with Tezpur University and together conducted a pilot to introduce and test the Fluoride Nilogon filter among 300 households at three villages in Al Musaymir district of Lahj governorate. Following the successful implementation, demonstrated efficacy and wider adoption of the filter in this initial phase, ZOA expanded the project to the Al Dhale'a governorate in a second phase with 400 household filters and 1 community filter at 2 villages in Al Azariq and Al Hussein districts. The intervention areas are shown in Fig. 1.

Here we report suitability study of four limestone samples, two each for phase I and phase II including detail characterization of the limestone, laboratory testing of suitability of the limestone to select the better ones in each phase complemented by performance in fluoride removal by the limestone samples in Fluoride Nilogon in series of laboratory defluoridation experiments. The evaluation of key physico-chemical properties, including porosity, density, and chemical impurities, is crucial in determining the suitability of limestone for the Fluoride Nilogon method of defluoridation as these properties are anticipated to significantly influence the efficiency of the method (Mohan and Dutta 2020b, 2020a). The resulting pH of the treated water, a critical parameter for water quality, was analysed.

2. Materials and methods

2.1. Materials

Limestone samples utilized in both phases of the study were collected by ZOA from a factory which supplies limestone distinct geological locations within the Lahj governorate of Yemen shown in Fig. 2. In Phase I, Sample A was collected from the Al Melah district, while Sample B was obtained from the Al Musaymir district, specifically in the proximity of the National Cement Company, Musaymir. In Phase II, Sample C was sourced from the same location as Sample B, but sourced after about two years. Additionally, Sample D was collected from the Al Wadi area, also within the Al Musaymir district. The limestones were affordable, and no fees were paid. However, for the supply and crushing of the stones for use in the filters in the villages, ZOA contracted with a supplier to execute this required work. The limestones were crushed in the factory according to a specific size and shape. Furthermore, ZOA couriered four samples of limestone to the Tezpur University in India to find out the most appropriate and suitable samples to be used during the activation and treatment. At Tezpur University, the crude limestones were crushed using a laboratory stone crusher and segregated with chip sizes between 0.5–1.0 cm using standard sieves for the suitability testing.

At Tezpur University, AR grade sodium fluoride (NaF) and phosphoric acid (PA) were obtained from Merck, Mumbai and used as such. Fluoride stock solution of 1000mgL^{-1} concentration was prepared by adding NaF in double distilled water. Using this stock solution, fluoride working solutions of 10mgL^{-1} concentration were prepared. Groundwater fluoride is usually within 10mgL^{-1} because groundwater fluoride is usually below 10mgL^{-1} . It may be mentioned here that fluoride removal by Fluoride Nilogon is independent of initial fluoride concentration up to 20mgL^{-1} (Gogoi et al., 2015; Mohan et al., 2020). Orion Ionplus® supplied total ionic strength adjustment buffer III (TISAB III) used. For using in the field in Yemen, phosphoric acid was not available in the local market, ZOA found some challenges to obtain this item in

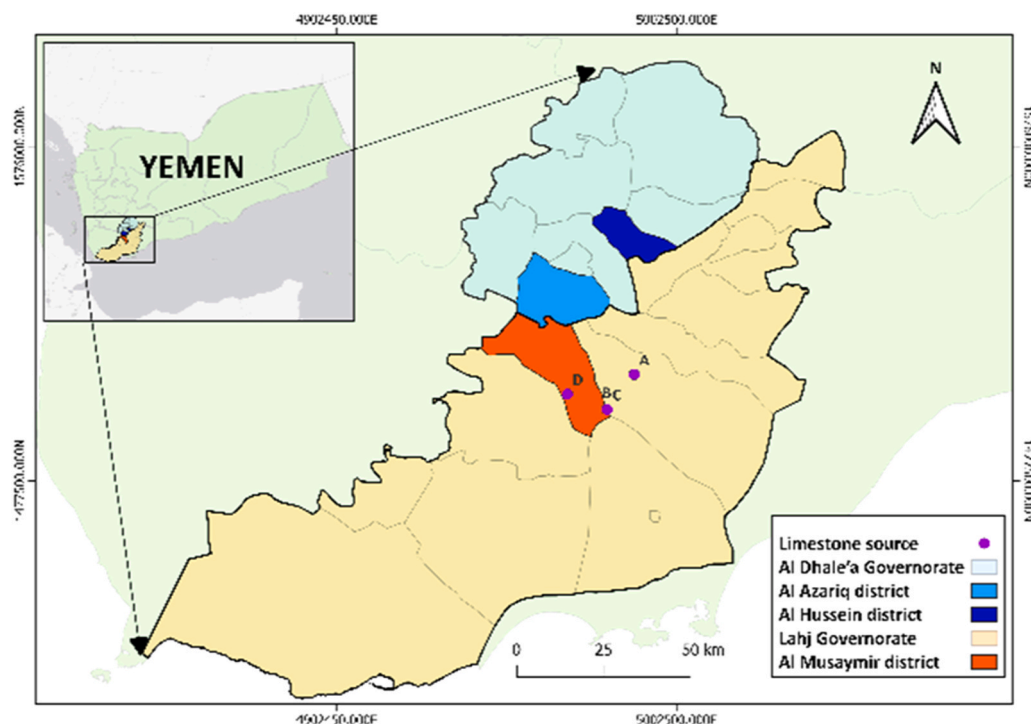


Fig. 1. Map of intervention areas in Yemen and the source locations of limestone samples used in the present study: A – from Al Melah district, B, C & D – from Al Musaymir district.



Fig. 2. Images of limestone samples A, B, C, and D used in the current study. Samples A and B were received in crushed form. Samples C and D were received as large pieces.

Aden city. However, phosphoric acid (Tech grade, CAS No. 7664–38–2) was finally obtained from a supplier in Sana'a, though there were additional difficulties due to the involvement of the de facto authorities (DFA) in that region.

2.2. Analytical methods

Four crude limestone samples (labelled A, B, C, and D) were crushed and then powdered for multi-technique characterization. Energy dispersive X-ray (EDX) spectroscopy was conducted using a JEOL JSM-6390LV scanning electron microscope (JEOL, Japan) operated at 15.0 kV under ambient conditions. Powder X-ray diffraction (PXRD) patterns were obtained using a Rigaku Miniflex diffractometer (Rigaku, Japan) with graphite-monochromated CuK α radiation ($\lambda = 0.15$ nm), operating at 30 kV and 15 mA with a scanning rate of 0.05°s^{-1} . Fourier

transform infrared (FTIR) spectra were recorded using a PerkinElmer Frontier NIR/FIR spectrometer in the $4000\text{--}400\text{ cm}^{-1}$ range with samples prepared in KBr pellets.

Surface area and porosity were evaluated via the Brunauer–Emmett–Teller (BET) method using an Autosorb iQ analyzer (Quantachrome, USA). The surface area of the sample was determined using nitrogen adsorption–desorption isotherms analyzed by the BET method. The BET equation, expressed as

$$(P/P_0)/[v(1-P/P_0)] = (C-1)/V_m \cdot C \cdot P/P_0 + 1/V_m \cdot C \quad (1)$$

(For N₂) $Sw = 4.36 \cdot V_m / \text{Mass}$, Single Point BET Equation ($C > 1$) and $V_m = V \cdot (1 - P/P_0)$ where, V is the volume of gas adsorbed at standard temperature and pressure (STP), V_m is the volume of gas required to form a monolayer, P is the equilibrium pressure of the adsorbate gas, P_0 is the saturation pressure of the adsorbate gas, C is the BET constant, related to the heat of adsorption.

Elemental composition was detected using Inductively Coupled Plasma Optical Emission Spectroscopy (ICP-OES) with a PerkinElmer Optima 2100DV (PerkinElmer, USA). For digestion (Turek et al., 2019), 1.00 g of each powdered sample was treated with a mixture of 12 mL concentrated HNO₃ and 4 mL concentrated HCl (Rate and McGrath, 2022), heated for 2 h in covered beakers on a hot plate. All solutions with undissolved residues were transferred into 100 mL volumetric flasks and filled to the mark with deionised water, followed by filtration.

The concentration of fluoride in the water samples were measured using a Multiparameter Kit (model: Orion Versastar pH-ISE-Cond-RDODO) with a fluoride ion-selective electrode (ISE) at the laboratory at Tezpur University for suitability testing and by SPADNS method using Palintest photometer MD600 in Yemen. TISAB III was added to these water samples before measuring fluoride concentration to decomplex the fluoride ions present in them. The pH was determined using an Orion Multiparameter Kit (Orion 5 Star pH-ISE-Cond-DO Benchtop) with a pH electrode at the laboratory at Tezpur University and was measured on a Milwaukee pH meter in Phase-I and WS 100 Potable Fluoride/ pH meter-F501-S3-in –1 Fluoride Electrode- Apera Device in Phase-II at Yemen. Testing of relevant water quality parameters of the untreated and

treated water in Yemen was done at the central laboratory for water analysis.

2.2.1. Procedure of study of fluoride removal ability of limestone

Batch experiments for fluoride removal were conducted using 2 L low-density polyethylene (LDPE) mug reactors filled with crushed limestone as described elsewhere (Mohan and Dutta 2020a). Groundwater was spiked with sodium fluoride (NaF) solution to adjust the fluoride concentration to 10mgL^{-1} . Measured volumes of 85 % w/v phosphoric acid (PA) were added to the groundwater to obtain the required PA concentrations, as PA is available in the market in 85 % w/v concentration. The composition of the groundwater is presented in supporting information (SI-1) (Das et al., 2025). Batch experiments were conducted to assess the fluoride removal capacity of limestone. The fluoride solution (10mgL^{-1}) and phosphoric acid were added to the mug reactors and allowed to react for predetermined residence time of 3 h. The residence time and the volume of water treated in a batch determine the quantity of water treated in a period. The first and the second batches, i.e., batch number 1 and 2 were for activation and treated with 0.01 M PA while batch number 3 onward were with the regular dose of 0.68 mM PA. After treatment, the solutions were filtered through Whatman No. 42 filter paper (Gogoi et al., 2015; Mohan et al., 2020).

2.2.2. Procedures for the field Fluoride Nilogon filters

2.2.2.1. Household Fluoride Nilogon filters in both phases. To ensure the proper installation and use of the filter by beneficiaries, ZOA trained local youth, both male and female, from the targeted areas. These youth educated beneficiaries on the importance of using the filter and trained them on how to install and use it daily. Additionally, there was a field supervisor to facilitate, follow up and monitor the field team. The Fluoride Nilogon filter consists of two buckets, with the top bucket containing crushed limestone that reacts with phosphoric acid and fluoride to lower the fluoride concentration in the water. The ZOA field team distributed filter materials. Each family received the following for setting up the household filters:

- (1) One 40 L plastic barrel
- (2) One 20 L plastic barrel
- (3) 60 kg of crushed limestone
- (4) One piece of thick white porous cloth
- (5) One 15 L plastic container for storing drinking water

60 kg of crushed limestone is required to fill the reactor container, i.e., to make the crushed limestone bed. The void volume in a 40 L drum filled with 60 kg crushed limestone is 15 L allowing to treat 15 L of water in each batch.

The families were also supplied with a bottle containing 1 L of 8.5 % PA which lasts for approximately 142 days if used for one batch per day or 71 days for two batches per day. The frequency of application of PA in household filters is usually once per day as fluoride-free water is required only for drinking and cooking purposes. Since measuring 7 mL of 8.5 % PA is more convenient for villagers than 0.7 mL of 85 %, the dose regular was decided as 8.5 % of PA for each batch of household Fluoride Nilogon for fluoride removal from 15 L water. Use of 8.5 % PA, though a weak acid, is also safer for the villagers than 85 % PA.

After crushing the limestone to the desired size and installing the tap at the bottom of the plastic barrel, place large-sized pieces of limestone at the bottom of the plastic barrel until the tap is covered from the inside. Then, the barrel with the smaller pieces of limestone should be filled to ensure that the tap does not become clogged with small pieces of limestone. Ultimately, ZOA delivered Fluoride Nilogon filters to the targeted locations in the governorates of Lahj in Phase I and of Al Dhale'a in Phase II. Altogether 700 household Fluoride Nilogon filters, as shown in Fig. 3, were installed at Lahj and Al Dhale'a governorates (Mohan and Dutta 2020a). The fluoride concentrations in water of the selected field sources were found to be in the range $2.8\text{--}20.0\text{mgL}^{-1}$. A schematic diagram with operational steps of the filter has been included in Fig. 3 along with pictures of both the laboratory setup and the field-based Fluoride Nilogon filters.

2.2.2.2. Community Fluoride Nilogon filter in phase II. For the community Fluoride Nilogon filter of total 18,000 L concrete reservoir filled

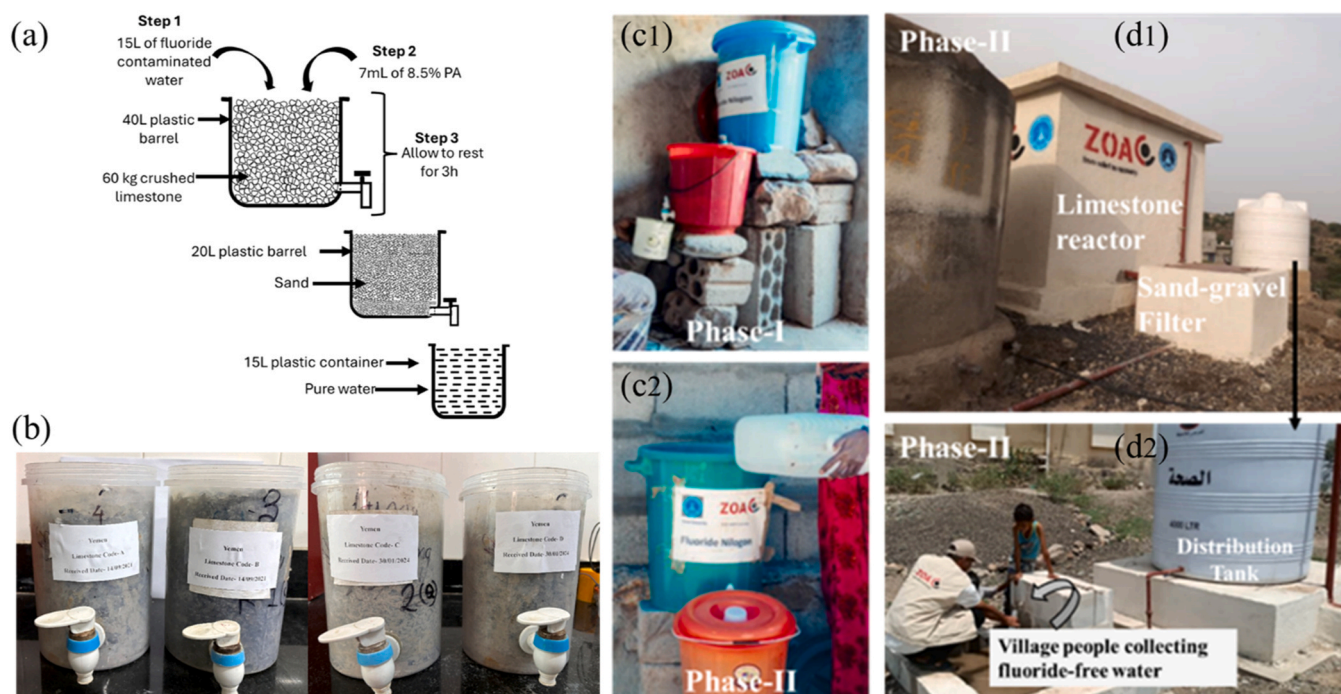


Fig. 3. (a) A schematic diagram of operational steps of Fluoride Nilogon, (b) the laboratory setup for suitability study, (c) field setup for two household Fluoride Nilogon filters installed in Phase-I and Phase-II, and (d) the reactor (1, top right) and the distribution unit (2, bottom right) of the community Fluoride Nilogon filter of Phase II.

with crushed limestone and sand as a reactor, purposed for the treatment of approximately 7000 L (void volume) of water per batch, was installed in Al Dhale'a governorate (Fig. 3). Sand serves in post-treatment filtration. It effectively removes suspended solids and turbidity from raw water including tiny fluorite particles, ensuring cleaner flow to the active limestone bed. The reactor chamber filled with crushed limestone of size 1–20 mm gave a void volume which able to treatment 7000 L of water. A plastic gallon was used for mixing PA into the fluoride-contaminated water and for feeding the reactor. Approximately 27,000 kg of crushed limestone was required to fill the 18,000 L size reactor. Activation of the reactor was conducted twice, once in a day, each time water containing 0.01 M phosphoric acid (PA) by added, 6.8 L of 85 % PA to 10,000 L of water or 68 L of 85 % PA to 100,000 L of water or 47.6 L of 85 % PA to 70,000 L of water. For community-level filters, there are no measurement or safety issues occurs as the dose is added by a trained and qualified person.

2.2.2.3. Activation of the crushed limestone reactors. The crushed limestone reactors of the household and the community Fluoride Nilogon filters were activated after their installations as per the procedure suggested by the Tezpur University team based on the suitability test conducted at Tezpur University laboratory described elsewhere (Mohan and Dutta 2020a, Nath et al., 2011; Gogoi et al., 2015; Mohan et al., 2020). ZOA provided the necessary materials and equipment to test the fluoride concentration in drinking water samples collected in the field and monitored the continuous decrease in fluoride concentration. To further ensure the quality of the work, the ZOA team installed filters in the office in Aden so that staff could verify the accuracy of the fieldwork by comparing the results with the results of the samples collected in the field. The doses of 0.01 M PA for activation and 0.68 mM for regular treatment were decided based on the suitability test for limestone samples described earlier (Gogoi et al., 2015; Mohan et al., 2020). The doses were verified for the limestone samples from Yemen at the laboratory at Tezpur University. The doses were also verified for Yemeni groundwater by the team in Yemen.

3. Results and discussion

3.1. Physicochemical characterization of the crude limestone samples from Yemen

The physicochemical characteristics of the limestone samples, A and B, which were collected for Phase I, and samples C and D, which were collected for Phase II, were examined to correlate with the fluoride removal ability of the crushed limestone by the Fluoride Nilogon method. The after-treatment characterization of limestone was reported earlier (Mohan and Dutta 2020a, Nath et al., 2011).

3.1.1. BET analysis

Based on the IUPAC classification of adsorption isotherms and the results obtained from nitrogen adsorption-desorption analysis at 77.35 K, all four samples exhibited characteristics corresponding to Type IV isotherms, which are typical for mesoporous materials (Fig. 4) (Abebe et al., 2018). Type IV isotherms are identified by the initial formation of a monolayer followed by multilayer adsorption, culminating in capillary condensation within mesopores. These isotherms often display a “sharp knee” and a hysteresis loop, indicating the transition from monolayer to multilayer adsorption and the presence of mesoporosity (Abebe et al., 2018).

Sample D exhibited the highest BET surface area of 1.447 m²/g and a total pore volume of 0.004 cm³/g, with an average pore diameter of 10.03 nm (Table 1). These properties suggest a well-developed mesoporous structure, potentially favourable for applications requiring higher adsorption capacity and accessible surface area. Sample B

Table 1

BET surface area, total pore volume, average pore diameter and density.

Sample Code	BET surface area (m ² /g)	Total pore volume (cm ³ /g)	Average pore diameter (Å)	Density g/cm ³
A	1.021	3.56×10^{-3}	124.3	2.75
B	1.267	3.24×10^{-3}	95.5	2.99
C	0.838	3.71×10^{-3}	149.0	2.22
D	1.447	4.08×10^{-3}	100.3	2.39

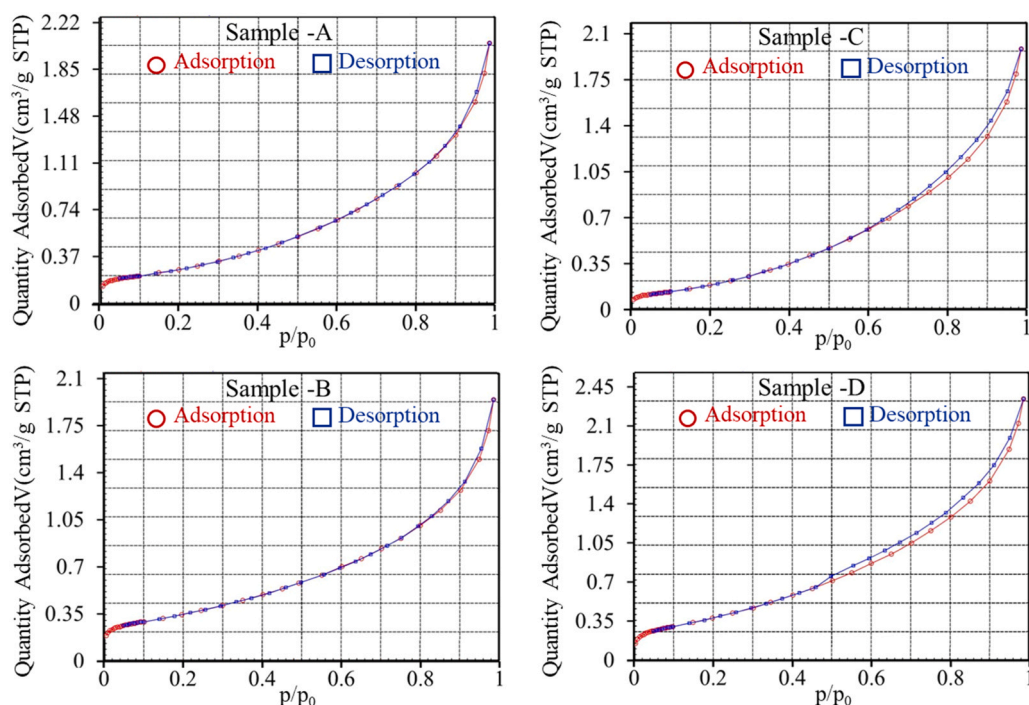


Fig. 4. BET adsorption isotherm plot of crude limestone samples A, B, C and D.

showed the second-highest surface area ($1.267 \text{ m}^2/\text{g}$) and a pore diameter of 9.55 nm , indicating relatively uniform mesoporosity. Sample A had a lower BET surface area of $1.021 \text{ m}^2/\text{g}$ and a pore size of 12.43 nm , while Sample C demonstrated the lowest surface area of $0.838 \text{ m}^2/\text{g}$ but with the largest pore diameter of 14.90 nm . The increase in pore diameter in Sample C may have contributed to reduced surface interactions, thereby lowering the overall surface area.

The density of each limestone sample was determined using the gravimetric method, applying the equation $\rho = M/V$, where ρ represents the density (g/cm^3), M is the measured mass of the dry sample (g), and V corresponds to the volume (mL) displaced by the sample in water using a graduated cylinder based on Archimedes' principle. This displacement method was employed to account for the irregular shapes of the limestone particles and ensure accuracy in volume determination (Table 1). Among the tested samples, Sample C exhibited the lowest density at $2.22 \text{ g}/\text{cm}^3$, followed by Sample D ($2.39 \text{ g}/\text{cm}^3$), Sample A ($2.75 \text{ g}/\text{cm}^3$), and Sample B, which showed the highest density at $2.99 \text{ g}/\text{cm}^3$. Thus, the order of increasing density is $C < D < A < B$. All measurements were carried out under ambient laboratory conditions at 25°C . The observed variation in density may be attributed to differences in mineralogical composition, porosity, and microstructural characteristics of the limestone samples, which can significantly influence their performance in adsorption-based fluoride removal processes.

The comparative analysis confirms that all samples fall within the mesoporous range ($2\text{--}50 \text{ nm}$), supporting their classification under Type IV isotherms. Among them, Sample D exhibits the most promising physicochemical properties for adsorption-related applications. For comparative representation and isotherm interpretation, plotting nitrogen adsorption-desorption isotherms (adsorbed volume vs. relative pressure, p/p_0) is recommended. These plots would visually affirm the mesoporous nature and Type IV behaviour of the materials, including the presence or absence of hysteresis loops, which further elucidates the pore structure and adsorption mechanism.

3.1.2. Elemental detection

Fig. 5 shows the analysis by ICP-OES for the elemental impurities of Al, Fe, Mn, Mg, K and Na in the limestone samples. The limestone samples collected in Yemen (A, B, and D samples) were characterised by their higher purity. Sample C had very high aluminium (Al), iron (Fe), manganese (Mn), potassium (K), magnesium (Mg), and sodium (Na) levels, as seen in Fig. 5, having a lower purity level than the other samples. These results are in accordance with those of Sdiri et al., where it was observed that impure limestones, especially those with greater content of silica, iron, and aluminium oxides, exhibited greater removal efficiencies compared to the less impure limestones (Sdiri et al., 2012). This implies that the content of impurities in sample C can contribute positively to adsorptive processes engaged in contaminant elimination.

Mohan et al. using PHREEQC to understand the effects of impurities like oxides of Fe and Al, commonly present as Fe_2O_3 and Al_2O_3 in

limestone. The PHREEQC program predicted that the presence of these metal oxides in any limestone can be a boon by helping in adjusting the final pH of the treated water at around 7.5 instead of 8.5 in the case of pure limestone and by contributing in fluoride removal. When Al_2O_3 and Fe_2O_3 were introduced in PHREEQC, with their concentrations being increased from 0.0001 M to 0.1 M , the predicted pH got reduced from 7.929 to 7.324 for Al_2O_3 and 7.930–7.339 for Fe_2O_3 . The program predicted an increase in the amount of CO_2 in the system from 6.88 to 125.80 mmol for Al_2O_3 and from 6.86 to 95.86 mmol for Fe_2O_3 , which may be a plausible cause for this decrease in pH, as carbon dioxide will react with water, forming carbonic acid. The presence of Fe and Al impurities in these limestone samples is also expected to cause crystal defects, facilitating dissolution of limestone and adsorption of fluoride, resulting in better fluoride removal (Mohan and Dutta 2020a). Additionally, Fe^{3+} can form FeF_3 complexes to assist fluoride removal, or stabilize HAP by maintaining pH within 6.5–8.5.

3.1.3. FTIR, PXRD and EDX analysis

The FTIR spectra of crude limestone samples A, B, C, and D (Fig. 6 (1)) showed typical vibrational bands for calcium carbonate. Sharp absorption peaks were invariably found in all samples at around $2531\text{--}2517 \text{ cm}^{-1}$, $1433\text{--}1429 \text{ cm}^{-1}$, $876\text{--}874 \text{ cm}^{-1}$, and $713\text{--}707 \text{ cm}^{-1}$, indicating the presence of carbonate functional groups and align well with previously reported data (Mohan and Dutta 2020b, 2020a). A wide absorption band of $3523\text{--}3437 \text{ cm}^{-1}$ was found present in all samples and has been assigned to O–H stretching vibrations, possibly from adsorbed atmospheric water or structural hydroxyl groups (Madejová 2003). The general spectral trends were found to be quite similar across the four samples A, B, C and D, reflecting similar chemical and mineral composition. Nonetheless, minor differences in peak intensities were observed, which could be caused by varying crystallinity, grain size distribution, or minor impurities like silica or clay minerals (Balan et al., 2001). The differences might be evidence of minimal variations in the geological origin, depositional environment, or post-depositional alteration processes of the limestone material.

The PXRD patterns of the powders of the limestone samples are depicted in Fig. 6(2). All the samples showed well-defined diffraction peaks for the crystalline calcium carbonate phases. Strong reflections were seen at 2θ values of 23.08° (102), 29.42° (104, strong intensity), 36.01° (110), 39.46° (113), 43.21° (202), 47.55° (108), and 48.53° (116), which are characteristics of the calcite polymorph of CaCO_3 (Mohan and Dutta 2020b). These observations verify the dominance of the calcite phase in every sample that was analysed. In addition, a very weak diffraction peak near $2\theta = 26.63^\circ$, corresponding to the (101) plane, was detected in samples C and D. This subtle peak suggests the presence of a minor quartz (SiO_2) phase in these samples, indicating a possible siliceous impurity or natural compositional variation within the limestone matrix.

The elemental composition of the limestone samples was analysed using EDX, with the results shown in Fig. 7. All samples revealed a high concentration of calcium (Ca), carbon (C), oxygen (O), and silicon (Si), indicating the dominant presence of calcium carbonate and silicate phases. Notably, in Phase II, sample C exhibited elevated iron (Fe) content, while sample D showed a higher aluminium (Al) concentration. In Phase I, sample B displayed a greater aluminium (Al) content compared to sample A. Although typically considered impurities, the presence of Fe and Al may positively influence the material's physicochemical properties under certain conditions. The presence of these elements aligns well with the structural and functional features identified through complementary FTIR and XRD analyses, reinforcing the reliability of the multi-technique characterisation approach.

3.2. Fluoride removal ability of limestone samples A, B, C, and D

For determining the fluoride removal efficiency of limestone samples under both Phase-I and Phase-II, the samples were treated with 0.01 M

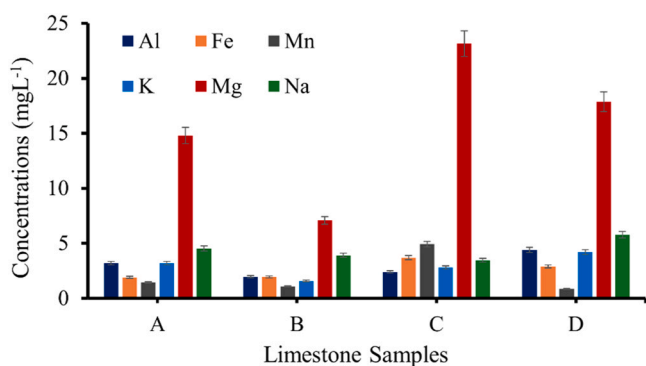


Fig. 5. Elemental, other than Ca, detection carried out at Tezpur University, in crude limestone samples A, B, C, and D received from Yemen.

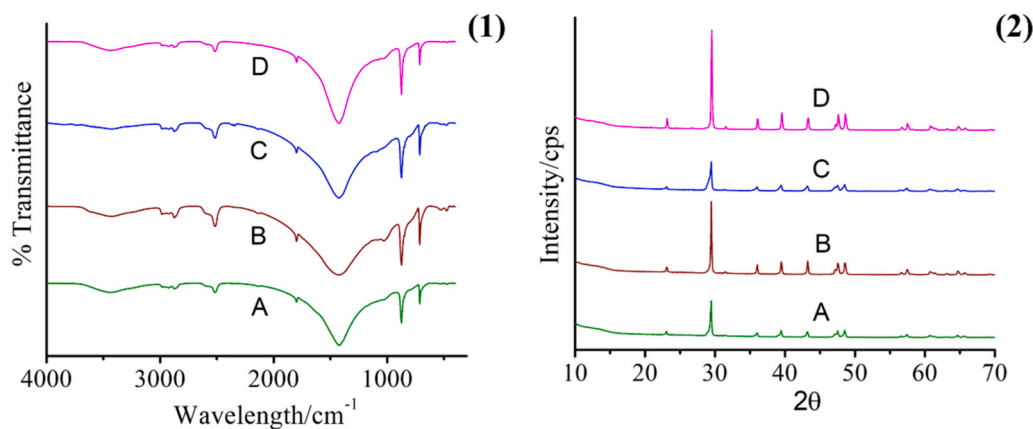


Fig. 6. The FTIR (1) and PXRD (2) spectra of crude limestone samples A, B, C, and D from Yemen.

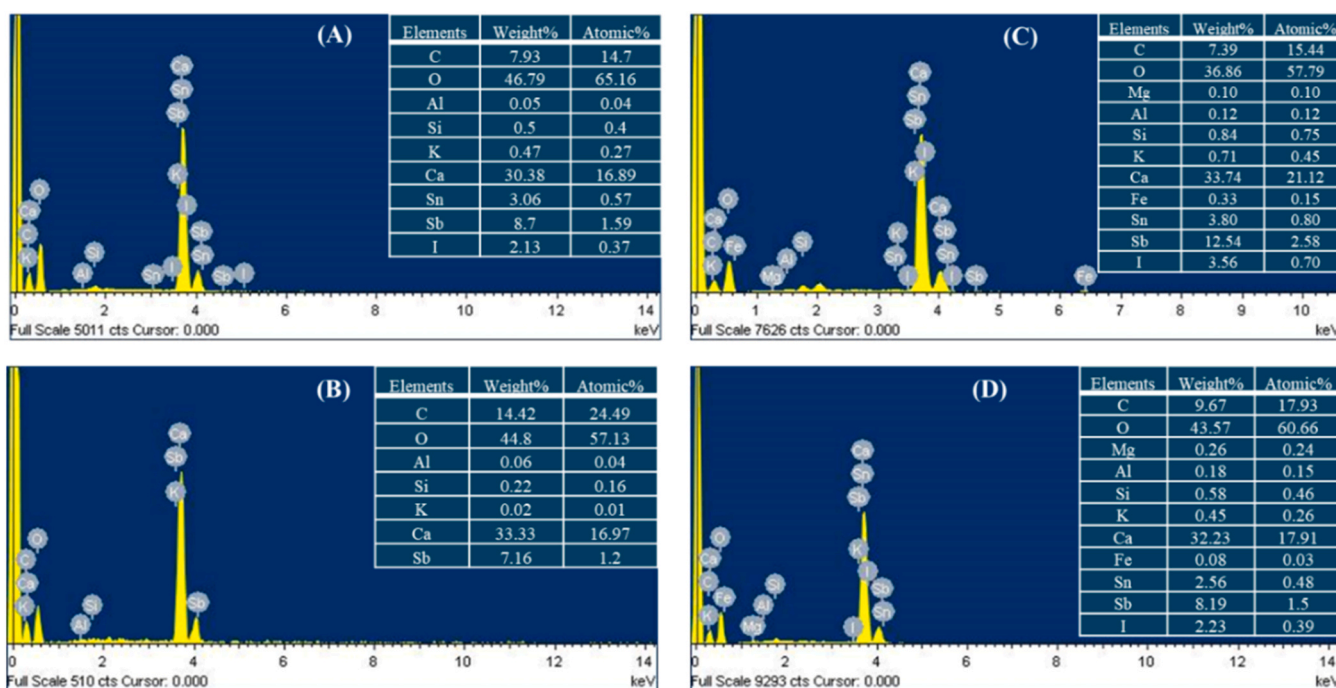
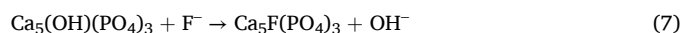
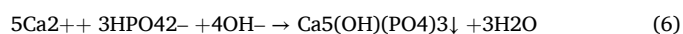
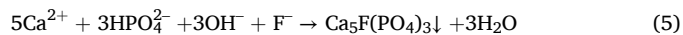
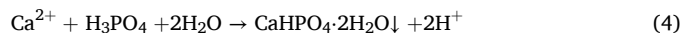
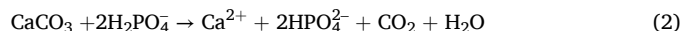
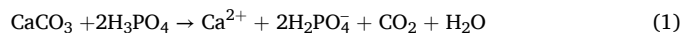


Fig. 7. The EDX spectra of crude limestone samples A, B, C, and D received from Yemen.

PA in the presence of 10mgL^{-1} of initial fluoride concentration, $[\text{F}^-]_0$. On subsequent treatments, the $[\text{PA}]_0$ concentration of 0.68 mM was used. The results are shown in Fig. 8. The removal of fluoride by limestone samples occurs through a combined mechanism of CaF_2 precipitation and hydroxyapatite (HAp)-mediated adsorption (Mohan and Dutta 2020a).

The removal of F^- by precipitation of CaF_2 is limited to $1\text{--}2\text{mgL}^{-1}$ by thermodynamic restriction, viz., solubility product of CaF_2 , which is $4.14 \times 10^{-11}\text{ mol}^3\text{L}^{-3}$ (Turner et al., 2005, Reardon and Wang, 2000). The precipitation, which otherwise is an instantaneous process, is slowed down to 3–4 min by slow dissolution of limestone by dilute PA. It is difficult to distinguish rapid precipitation and adsorption in Fig. 8 as we have only the equilibrium data. The CaF_2 precipitate formed in the treated groundwater remains in the limestone bed. The precipitate neither reduce fluoride removal during subsequent treatment batches nor it does any clogging of water. However, the dominant mechanisms have been discussed in previous reports from this group (Gogoi and Dutta, 2016; Gogoi et al., 2015) with illustration of saturation index of CaF_2 .

The reactions involved in Fluoride Nilogon process have been summarized (Mohan et al., 2020):



Among the limestone samples, B, C, and D exhibited a more rapid precipitation driven fluoride removal compared to sample A. This trend suggests a greater capacity for fluorite formation in these samples, potentially due to variations in mineralogical composition. Previous findings by Mohan et al. support this observation, indicating that the

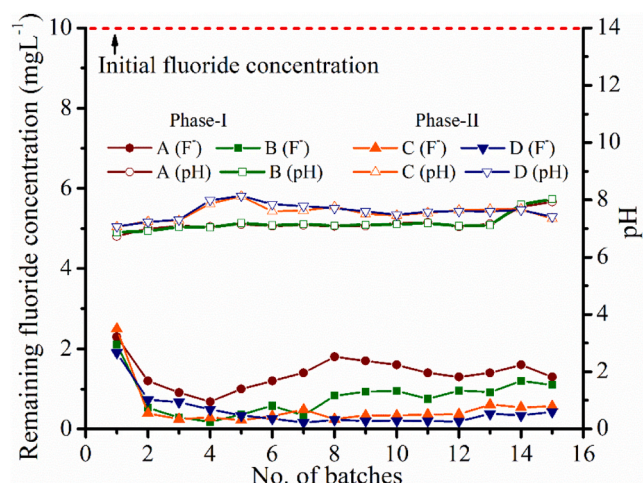


Fig. 8. Results of PACLT for suitability test using an initial fluoride concentration of 10mgL^{-1} for Phase I (samples A and B) and Phase II (samples C and D). $[\text{PA}] = 0.01\text{ M}$ for batches 1–3 and 0.68 mM thereafter. Closed and open symbols are for remaining $[\text{F}^-]$ and corresponding pH of water after treatment.

presence of metal oxides such as Al_2O_3 and Fe_2O_3 , frequently detected in limestone, can enhance defluoridation by modulating the solution pH and promoting both fluorite precipitation and in situ HAP formation, as predicted using PHREEQC simulations (Mohan and Dutta 2020a). The variation in pH as a function was measured for the treated water and shown in Fig. 8 of secondary Y-axis. The initial pH of the untreated water containing 10mgL^{-1} of fluoride and 0.68 mM $[\text{PA}]_0$ was 5.78. A rapid initial increase in pH was observed due to the first and second deprotonation of weak acid PA, which finally completes in 3 h, and the pH levels off. The final pH of the treated water in A, B, C, and D was in the range of 6.5–8.5 as prescribed by BIS (Bis, 2012). The pH variation with time has been discussed in our previous reports (Nath and Dutta, 2010; Gogoi et al., 2015; Gogoi and Dutta, 2016), with the last paper focusing on the mechanism of PACLT alone. The observed pH shift from initial acidity (pH ~5.78) to neutrality (pH 6.5–8.5) plays an important role the mechanism in the PACLT method. The initial acidic conditions are crucial for dissolving the limestone (CaCO_3), thereby releasing calcium ions (Ca^{2+}) into the solution, which initiates the precipitation reaction. The total dissolved solids (TDS) before and after PACLT treatment were 150mgL^{-1} and 230mgL^{-1} , respectively, indicating an increase in TDS due to the influence of PA addition. Similar observations were reported earlier from a field experiment (Mohan et al., 2020).

3.3. Field experience

3.3.1. Intervention areas

The intervention areas of both phases are given in Table 2. In Phase I, ZOA targeted 300 households Fluoride Nilogon filters across three villages in Lahj governorate for fluoride mitigation where the groundwater fluoride is 3.1mgL^{-1} . In Phase II, 400 household Fluoride Nilogon filters were installed in Khoubur village, Al Hussein district, along with a

community-scale filter unit of 18,000 L total volume and 7000 L void volume or capacity of water treatment in a batch. The community filter was aimed to cater for 100 households in Habel Ghabas village, Al Azariq district, Al Dhale'a governorate, in response to severe health concerns linked to chronic fluoride exposure. In Khoubur village, residents report various health issues, including dental and skeletal fluorosis, arthritis, and other musculoskeletal disorders. The fluoride concentrations in the groundwater in these areas have alarmingly exceeded the WHO's recommended limit of 1.5mgL^{-1} , reaching levels between 9.3mgL^{-1} and 10.5mgL^{-1} .

3.3.2. Design and cost

Designed for simplicity and effectiveness, the system effectively reduces fluoride levels within three hours. The recurring operational costs are minimal, mainly requiring a daily addition of a small quantity of phosphoric acid.

The detail life cycle cost of Fluoride Nilogon was already reported (Mohan et al., 2020). From the field results, it was clear that the limestone should work for at least a lifetime without needing replacement, replenishment, or regeneration until it is totally dissolved by the tiny quantity of PA added in every batch (Mohan et al., 2020). The estimated life of the crushed limestone bed of a household Fluoride Nilogon unit used twice a day with up to 20mgL^{-1} feed water is 39,210 batches or over 50 years. For estimating the recurring cost of Fluoride Nilogon, only the cost of phosphoric acid (PA) is considered

For Fluoride Nilogon in Yemen, household water filtration units have a capital expenditure of USD 15 and an operational expenditure of USD 0.00063 per L, as only PA is needed and no manpower cost is involved. The capital expenditure of the 7000 L community filter was USD 18,000. The operational expenditure of the community filter has been estimated as USD 0.000293 per L, which accounts for USD 0.00023 and USD 0.00063 as the cost of manpower and of PA, respectively. These recurring costs are significantly lower than that of reverse osmosis (\approx USD 0.0061, considering USD 68.21 annual maintenance for 30 L daily consumption) and other adsorption-based fluoride removal filters (Mohan et al., 2020).

3.3.3. Setting up of the field Fluoride Nilogon filters

Fluoride removal efficiency was systematically assessed in two implementation phases under varying contamination conditions. In Phase I, household filters were deployed in areas with moderate fluoride levels, where the influent water exhibited an average concentration of 3.2mgL^{-1} . Regular monitoring of both influent and effluent samples demonstrated that all filters consistently reduced fluoride concentrations to levels below the WHO guideline of 1.5mgL^{-1} , indicating stable and effective performance in field settings. The average value of the fluoride concentration in the effluent water from 300 filters were found to be $< 1.0\text{mgL}^{-1}$.

3.3.3.1. Selection of limestone samples for field use. From Phase I experiments, both samples A and B initially demonstrated effective fluoride removal. However, sample B maintained consistent performance over multiple batch cycles. This consistency correlates with earlier characterisation data (XRD, EDX, and BET analyses), which suggested

Table 2

Areas of intervention of fluoride removal from drinking water in Yemen in Phases I and II.

Phase	Governorate	District	Village	Filter type	No. of families	
					Targeted	Benefited
Phase I 2022	Lahj	Al Musaymir	Fara's Al Lojmah Al Oqma	Household	300	300
Phase II 2024	Al-Dhale'a	Al Hussein	Khoubur	Community	100	100
		Al Hussein	Khoubur	Household	300	325
		Al Azariq	Habel Ghabas		100	75

that sample B possessed superior textural and compositional features favouring adsorption. As a result, sample B was selected for subsequent field trials in phase I. From Phase II, samples C and D both showed excellent fluoride removal capabilities. Detailed physicochemical analyses revealed that sample C exhibited more favourable properties, like lower density and appropriate elemental composition, indicating a potentially higher adsorption efficiency than sample D. Based on these findings, sample C was chosen for field validation.

3.3.4. Activation and field performance of Fluoride Nilogon filters

The process of using the Nilogon filter is divided into two main stages: firstly, activation of the limestone and secondly, regular treatments to remove fluoride from drinking water. It was observed that, in the cases of all limestone samples, the effluent fluoride levels were $1.9\text{--}2.5\text{mgL}^{-1}$ and $0.39\text{--}1.2\text{mgL}^{-1}$ after the first and second batches, respectively, with 0.01 M PA (Fig. 8). As the effluent fluoride concentrations were below the desired level after the second batch, it was decided to carry out activation of limestone in the field reactors only twice with 0.01 MPA . The activation of limestone was carried out accordingly in two batches, once in a day for two days, with a dose of 0.01 MPA .

3.3.4.1. Performance of household filters in phase I. Table 3 shows [F⁻] in treated water samples from 10 household Fluoride Nilogon filters from the villages during regular use with 0.68 mM PA , after the activation. Samples of inflow and outflow have been taken at different weeks after installation of the filters to test the consistency of fluoride removal from the drinking water by the household filters installed in Phase I. The samples were collected once in a week for four weeks though the filter was used usually once in a day. All treated water samples collected from the filters from Lahj governorate up to four weeks showed fluoride concentrations within WHO guideline value of 1.5mgL^{-1} for safe drinking water reduced from the initial source-water fluoride concentration of 3.2mgL^{-1} (Table 3). The results were verified in the laboratory in treated water samples at a demo Fluoride Nilogon filter at ZOA office for four samples. It is evident from the table that all treated water had remaining fluoride concentrations below the WHO guideline value. The performances of the filters were therefore consistent as expected (Mohan et al., 2020).

3.3.4.2. Performance of household filters in phase II. In Phase II, the activation of the reactors of the household Fluoride Nilogon filters was done in the villages using the same dose 0.68 mM , by adding 7 mL of 8.5 \% PA to 15 L of water, for convenience. It was convenient to do so because in that case PA from the same bottle of PA supplied to users for regular use could be used for activation also. Table 4 shows the remaining [F⁻] of the treated water from 10 representative household Fluoride Nilogon filters for 7 batches, once a batch a day from 11 July to 17 July 2024, from the villages in Phase II in Al Dhale'a in Phase II. The remaining fluoride concentration showed almost gradual decreases each day. The fluoride concentrations, except filter No. 3, were below the WHO guideline value after the 7th batch. Filter No. 3 is also expected to

Table 3

Fluoride concentrations in the treated water samples collected in four weeks from the filters installed in Lahj governorate in Phase I, with source-water fluoride concentration of 3.2mgL^{-1} .

Sample source	Weeks	No. of samples from different filters	Remaining [F ⁻] range in mgL^{-1} *
Field filters	1	10	$1.09\text{--}1.36$
	2	10	$1.34\text{--}1.48$
	3	10	$0.89\text{--}1.45$
	4	10	$1.12\text{--}1.40$
ZOA office, Aden	-	4	$0.70\text{--}1.20$

*WHO guideline value 1.50mgL^{-1}

comply with the WHO guideline value within one or two batches, as indicated by the gradual decrease after each batch. There were some inconsistencies in the equilibrium fluoride concentrations for different source water and limestone reactors but all results in individual rows almost gradually decreased to finally comply with WHO guideline on the 7th day.

An untreated groundwater source sample from Al-Dale'a governorate along with six other treated groundwater samples after treatment by different Fluoride Nilogon filters were tested for some other relevant water quality parameters, namely pH, conductivity (EC) and total dissolved solids (TDS), etc. The results of the testing at Aden Water Supply Local and Sanitation Corporation laboratory are shown in Table 5. The pH of the untreated groundwater sample B was 7.03 , almost neutral. After treatment, the pH increased slightly to the range from 7.37 to 7.49 , indicating a moderate rise in alkalinity, except sample A2. The EC of the untreated groundwater was found at $1935\mu\text{S/cm}$, which decreased after treatment to $1813\mu\text{S/cm}$ to $1866\mu\text{S/cm}$ indicating removal of some conducting ions through precipitation, except sample A2. Similarly, the TDS in the untreated sample B was recorded at 1258mgL^{-1} , which after treatment decreased to the range of 1178mgL^{-1} to 1213mgL^{-1} , except for sample A2 where the TDS increased to 1489mgL^{-1} . The undesired results in the sample A2 may be attributed to presence of some alkaline impurity in the limestone which leads to increased bicarbonate in the treated water, which however is expected to be normal after regular use. However, all TDS, though very high were within the maximum permissible limit for drinking in Yemen. It is also interesting to note that the TDS and EC decreased to be more suitable for drinking after treatment in most cases while the pH also came closer to the middle of the acceptable range for drinking, i.e., $6.5\text{--}8.5$ prescribed by BIS (Bis, 2012).

3.3.4.3. Performance of the community filter in Phase II. The novel community-level filter was set up a community Fluoride Nilogon water treatment system to target 100 households in Khoubur village in Al Hussein district in Al Dhale'a governorate in Yemen. By the side of the community water tank, there were two water points, one for the inlet pumping of water and another for the distribution pipelines. The results of fluoride removal by the community filter for six successive days are shown in Table 6. The community water treatment system provides safe drinking water to 700 residents across Khoubur village in Al Dhale'a governorate in Yemen. The positive impact of this water treatment unit on the community is significant, providing a direct and sustainable solution for their water needs. The target area was provided with two plastic tanks, each of 4000 L capacity, and each containing a water distribution point consisting of two taps to obtain treated water.

3.3.4.4. Summary performance of filters in Phase I & II. Fig. 9 illustrates the results of comparing the untreated and treated water of household and community filters. In Phase II, the Fluoride Nilogon filters treated water with much higher initial fluoride concentrations averaging 10.5mgL^{-1} compared to 3.2mgL^{-1} of Phase I. Despite the elevated contamination, the filters achieved substantial fluoride removal, with all effluent samples very well meeting the WHO guideline of 1.5mgL^{-1} like those of Phase I. The Fluoride Nilogon filter improved groundwater quality by slightly increasing pH and reducing EC and TDS in most samples making the water better for consumption in terms of these parameters also. The observed better overall fluoride removal performances of the filters in the Phase II than in the Phase I may be attributed to the better suitability of the limestone used in the Phase II than that in the Phase I. These findings collectively confirm the robustness, reliability, and adaptability of the filtration systems across a range of fluoride exposures, supporting their suitability for deployment in both moderately and severely affected regions.

3.3.5. User training, feedback, and challenges encountered

Effective community engagement was essential to the successful

Table 4

[F] in the treated water on the 7th day/batch from 10 representative household Fluoride Nilogon filters from the villages in Phase II in Al Dhale'a governorate.

Household filter No.	Source [F] / (mgL ⁻¹)	[F] / (mgL ⁻¹) after treatment with 0.68 mM PA*						
		Day 1	Day 2	Day 3	Day 4	Day 5	Day 6	Day 7
1	11.19	5.47	3.97	3.49	3.46	3.39	0.61	0.45
2		7.39	8.30	6.48	3.80	1.73	1.46	0.98
3		8.33	8.68	6.13	5.61	2.45	2.66	1.57
4	9.31	7.92	7.56	6.49	4.40	3.81	1.15	1.36
5		6.59	6.44	4.74	4.67	3.32	1.09	1.12
6		8.47	8.49	6.23	3.38	3.63	2.41	1.07
7	10.45	8.11	5.87	5.47	4.45	3.97	0.93	0.91
8		7.73	6.74	4.88	5.11	4.46	2.87	1.02
9		4.16	4.07	3.97	2.70	2.31	1.76	1.41
10		6.07	4.35	4.34	3.02	3.28	1.96	0.68

*The experiments were carried out one batch in a day from July 11 to July 17, 2024

Table 5

Some relevant water quality parameters, viz., pH, EC and TDS, of an untreated groundwater sample along with those of six other samples treated by different Fluoride Nilogon filters in Al Dhale'a governorate.

Sample Name		pH	EC / (μs/cm)	TDS / (mgL ⁻¹)
Before Treatment	B	7.03	1935	1258
After Treatment	A1	7.37	1866	1213
	A2	8.55	2290	1489
	A3	7.34	1824	1186
	A4	7.49	1813	1178
	A5	7.47	1837	1194
	A6	7.49	1850	1203
BIS limits (Bis, 2012)	Acceptable Limit	6.5–8.5*	-	500
	Permissible limit	-	-	2000
Yemen guidelines (Bamsaoud and Saeed, 2021; Yemeni, 2006)	Min	6.5	-	-
	Max	9.0	2500	1500
WHO guideline value ⁵	-	-	1000	1000

*Acceptable range

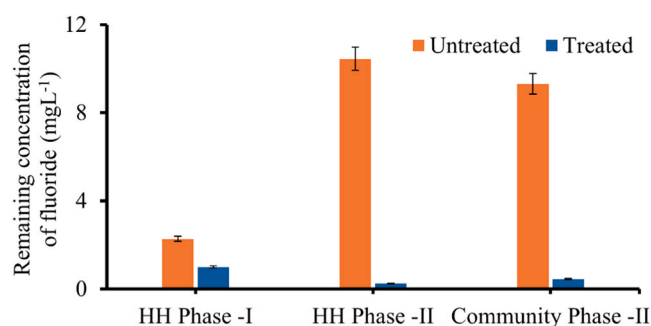
Table 6

Remaining fluoride during regular treatment in the community, Fluoride Nilogon filter after activation in Al-Al Dhale'a governorate, recorded for 6 batches once a day from 11 July to 16 July 2024.

Sl. No. of batch	[F] / (mgL ⁻¹) before treatment	Activation / Regular treatment	Initial [PA] / (mM ⁻¹)	Day	[F] / (mgL ⁻¹) after treatment
1	9.31–10.45* (As measured in two wells)	Activation	10	Day 1	0.85
2				Day 2	0.67
3				Day 3	2.68
4		Regular use	0.68	Day 4	1.47
5				Day 5	1.06
6				Day 6	0.97

installation of the filters. Awareness campaigns, training on filter maintenance, and educational workshops on fluorosis prevention and the safe use of phosphoric acid were conducted by ZOA Yemen. Pre-installation awareness sessions helped dispel misconceptions and ensured that beneficiaries participated in an informed and proactive manner.

Whereas 54 % of Phase I households used treated water solely for drinking purposes, most still utilised untreated water for cooking and

**Fig. 9.** Performance of household and community Fluoride Nilogon filters before and after treatment in terms of average effluent [F] in Phase I, and Phase II.

thus may have been contributing to continued fluoride intake. This highlights the importance of encouraging the domestic use of treated water for all household purposes. At the initial stage, some of the users were hesitant to add PA to drinking water, suspecting its adverse health effect. However, they later understood that PA is a weak edible acid and is also used in soft drinks and for food preservation. Community awareness on fluoride health risks was done by ZOA Yemen in both phases. Most respondents demonstrated an understanding of fluoride toxicity and were able to identify symptoms of chronic exposure, especially among vulnerable groups such as children.

User engagement with the filters was consistently high across both phases as was assessed through user feedback by ZOA Yemen. In Phase I, 98 % of recipient households reported daily use of the filters due to ease of operation and convenience. Phase II experienced even greater adoption, with 99 % of households actively using the filters and following the training guidelines. User feedback overall was extremely favourable, with 99 % rating the filters as good, very good, or excellent both in performance and usability.

3.3.6. Technical and operational challenges

The work in the field and in Yemen in both phases was challenging due to political instability and a war-like situation existing in Yemen. There were difficulties in road communication from the ZOA office in Aden to the villages as well as internet communication, especially between ZOA Yemen and Tezpur University. The internet communication was totally disrupted once for some time due to bombing at the internet hub in Yemen during Phase I.

During Phase I, following the initial activation of the limestone filtration system, fluoride levels unexpectedly increased rather than decreased. Investigations showed that the fluoride concentration in the treated water increased due to leaching of fluoride from the sand of the sand filter. The sand, which was initially used was reddish sand and was suspected to have fluoride impurity. So, the sand of the filters was

replaced with clean grey-white sand, and the problem was solved.

Another issue reported by the users was the occasional unavailability of phosphoric acid for replenishment, mentioned by 32 % of households, primarily due to delays in distribution. But this had no major impact on the system's overall functionality. However, another challenge now appears to be the continued supply of PA to the users as it is very difficult to get PA in the war-torn country due to absence of normal trade of neighbouring countries with Yemen. Even though some companies are ready to provide PA free of cost, it is difficult to find a transporter from a neighbouring country. However, PA is available in Yemen for about USD 100 per 35 kg of 85 % PA. COLA industries in Yemen are using PA as an ingredient for their soft drink products. Fluoride Nilogon gives safe drinking water not only by removing excess fluoride but also by improving potability of the water in terms of some more relevant water quality parameters like TDS. With a very low recurring cost of only a tiny quantity of PA, no requirement of any maintenance, and a life-time of the crushed-limestone bed (Gupta et al., 2021; Mohan et al., 2020), the issue of sustainability of the filters now is not of any scientific or technological performance but of improved political and commercial situations.

4. Conclusions

A total of 700 household (HH) and a community Fluoride Nilogon filters, based on phosphoric acid-crushed limestone treatment (PACLT), were installed in water-strained Yemen as a low-cost intervention to the severe fluoride contamination of drinking groundwater by ZOA, an international NGO with technology and technical support from Tezpur University (TU). It was implemented in two phases, with 300 HH filters at Farás, Al Lojmah, and Al Oqma villages in Al Musaymir district of Lahj governorate in 2021 catering safe water for 300 families in Phase I. Encouraged by the success of Phase I, 325 HH filters to cater for an equal number of families and a community Fluoride Nilogon filter of 7000 L water capacity to cater for another 100 families at Khawber village in Al Hussein district and another 75 HH filters to cater for another 75 families were installed at Habel Ghadas village in Al Azariq district, all in Al Dhale'a governorate in Yemen in Phase II in 2024. Suitability of two limestone samples, for each Phases, from sources from Musaymir district in Lahj governorate in Yemen were examined at TU. Based on physicochemical properties of the limestone complemented by the fluoride removal abilities by the limestones, one sample was selected for using in each phase though both samples examined for the Phase II were found to be almost equally suitable. The limestone samples examined for Phase II had more favourable porosity and Fe-Al impurity, along with much better fluoride removal ability compared to those for Phase I.

The average initial fluoride concentrations were 3.2mgL^{-1} and 10.5mgL^{-1} in Phase I and Phase II, respectively. The fluoride concentrations of treated water samples from all 700 HH and one community Fluoride Nilogon filters conformed to the WHO guideline of 1.5mgL^{-1} for fluoride. In addition to that, Fluoride Nilogon filters were also found to improve TDS, electrical conduction, and pH to make the water more suitable for drinking. The Fluoride Nilogon proved technically feasible and well-accepted by users by consistently reducing fluoride concentrations from as high as 11.19mgL^{-1} to below the WHO guideline of 1.5mgL^{-1} in both household and community levels. Initial challenges, including fluoride leaching from sand and occasional phosphoric acid shortages, were resolved without major impact on system performance. High daily usage and positive user feedback indicate strong engagement, driven by effective training and awareness programs, highlighting its potential for wider deployment in fluoride-affected areas of Yemen to ensure safe, sustainable access to drinking water.

CRediT authorship contribution statement

Bereket Godifay Kahsay: Visualization, Investigation. **Saranga Baishya:** Formal analysis, Data curation. **Gerrianne Pennings:**

Visualization, Investigation. **Tushmita Das:** Writing – original draft, Methodology, Investigation, Formal analysis, Data curation. **Harm Bouta:** Investigation, Funding acquisition, Conceptualization. **Anwesha Chaliha:** Data curation. **Matthijs T. Wessels:** Writing – review & editing, Visualization, Project administration, Investigation. **Priya Devi:** Data curation. **Sara Bazarah:** Visualization, Investigation. **Dutta Robin Kumar:** Writing – review & editing, Validation, Supervision, Resources, Funding acquisition, Conceptualization. **Amal Hasan:** Visualization, Investigation. **Wasim Al Shehab:** Visualization, Investigation. **Ham-mam Mukred:** Visualization, Investigation. **Saleh Radhwan Moham-med:** Visualization, Investigation. **Melhani Akram Al:** Visualization, Investigation. **Mohammed Riyadh:** Visualization, Investigation.

Declaration of Competing Interest

The authors declare that they have no conflict of interest.

Acknowledgements

The authors wish to thank the Mitswah Foundation for financially supporting both phases of the pilot fluoride removal projects.

Data availability

Data will be made available on request.

References

- Abebe, B., Murthy, H.A., Amare, E., 2018. Summary on adsorption and photocatalysis for pollutant remediation: mini review. *J. Encapsulation Adsorpt. Sci.* 8 (4), 225–255. <https://doi.org/10.4236/jeas.2018.84012>.
- Ahmad, S., Singh, R., Arfin, T., Neeti, K., 2022. Fluoride contamination, consequences and removal techniques in water: a review. *Environ. Sci. Adv.* 1 (5), 620–661. <https://doi.org/10.1039/D1VA00039J>.
- Al-Amry, A.S., Habtoor, A., Qatan, A., 2020. Hydrogeochemical characterization and environmental impact of fluoride contamination in groundwater from Al-Dhala basin. *Yemen EJUABA* 1 (1), 30–38.
- Al-Hmami, A., Jamaa, N.B., Kharroubi, A., Agoubi, B., Alwabr, G.M., 2024. Case-control study of drinking water quality in Yemen. *EMHJ East. Mediterr. Health J.* 30 (3), 212–220.
- Amini, M., Mueller, K.I.M., Abbaspour, K.C., Rosenberg, T., Afyuni, M., Möller, K.N., Sarr, M., Johnson, C.A., 2008. Statistical modeling of global geogenic fluoride contamination in groundwaters. *Environ. Sci. Technol.* 42 (10), 3662–3668. <https://doi.org/10.1021/es071958y>.
- Aqeel, A., Al-Amry, A., Alharbi, O., 2017. Assessment and geospatial distribution mapping of fluoride concentrations in the groundwater of Al-Howban Basin, Taiz-Yemen. *Arab. J. Geosci.* 10 (14), 312. <https://doi.org/10.1007/s12517-017-3069-y>.
- Arab, N., Derakhshani, R., Sayadi, M.H., 2024. Approaches for the efficient removal of fluoride from groundwater: A comprehensive review. *Toxics* 12 (5), 306. <https://doi.org/10.3390/toxics12050306>.
- Baghel, A.M., 2015. Prevalence of dental fluorosis in area of Yemen with above optimal level of fluoride in drinking water: An exploratory survey. *RRJoD* 6, 15–25.
- Balan, E., Saitta, A.M., Mauri, F., Calas, G., 2001. First-principles modeling of the infrared spectrum of kaolinite. *Am. Min.* 86 (11–12), 1321–1330. <https://doi.org/10.2138/am-2001-11-1201>.
- Bamsaoud, S.F., Saeed, F.F.B., 2021, May. Physical and chemical characteristics of Assaiq and Senah hot springs water in Hadhramout-Yemen and the assessment of water quality for drinking and irrigation purposes. In: *J. Phys. Conf. Ser.*, 1900. IOP Publishing, 012011. <https://doi.org/10.1088/1742-6596/1900/1/012011>.
- Bis, I. 10500 Indian standard drinking water-specification, second revision, Bureau of Indian Standards, New Delhi, 2012.
- Costantini, M., Colin, J., Decharme, B., 2023. Projected climate-driven changes of water table depth in the world's major groundwater basins. *Earths Future* 11 (3), e2022EF003068. <https://doi.org/10.1029/2022EF003068>.
- Crini, G., Lichtfouse, E., 2019. Advantages and disadvantages of techniques used for wastewater treatment. *Environ. Chem. Lett.* 17 (1), 145–155. <https://doi.org/10.1007/s10311-018-0785-9>.
- Das, T., Baroi, S., Saikia, R., Dutta, R.K., 2025. A hybrid method for simultaneous removal of hexavalent chromium and fluoride from drinking water in plug-flow mode. *J. Sep. Sci.* 60 (2), 220–233. <https://doi.org/10.1080/01496395.2024.2430639>.
- Gogoi, S., Dutta, R.K., 2016. Mechanism of fluoride removal by phosphoric acid-enhanced limestone: equilibrium and kinetics of fluoride sorption. *Desalin. Water Treat.* 57 (15), 6838–6851. <https://doi.org/10.1080/19443994.2015.1010592>.
- Gogoi, S., Nath, S.K., Bordoloi, S., Dutta, R.K., 2015. Fluoride removal from groundwater by limestone treatment in presence of phosphoric acid. *J. Environ. Manag.* 152, 132–139. <https://doi.org/10.1016/j.jenvman.2015.01.031>.

- Gourai, M., Nayak, A.K., Nial, P.S., Satpathy, B., Bhuyan, R., Singh, S.K., Subudhi, U., 2023. Thermal plasma processing of *Moringa oleifera* biochars: adsorbents for fluoride removal from water. *RSC Adv.* 13 (7), 4340–4350. <https://doi.org/10.1039/D2RA07514H>.
- Gupta, A., Knight, J., Greggio, E., Hosken, A., Addressing high fluoride water supply with an integrated mitigation programme – a case study, @WaterAid 2021, 1-7. (<https://washmatters.wateraid.org/sites/g/files/jkxoo256/files/202107/Case%20Study%203%20India%20DIGITAL.pdf>).
- Madějová, J.J.V.S., 2003. FTIR techniques in clay mineral studies. *Vib. Spectrosc.* 31 (1), 1–10. [https://doi.org/10.1016/S0924-2031\(02\)00065-6](https://doi.org/10.1016/S0924-2031(02)00065-6).
- Mohan, R., Dutta, R.K., 2020b. Continuous fixed-bed column assessment for defluoridation of water using HAP-coated-limestone. *J. Environ. Chem. Eng.* 8 (4), 103840. <https://doi.org/10.1016/j.jece.2020.103840>.
- Mohan, R., Dutta, R.K., 2020a. A study of suitability of limestone for fluoride removal by phosphoric acid-crushed limestone treatment. *J. Environ. Chem. Eng.* 8 (6), 104410. <https://doi.org/10.1016/j.jece.2020.104410>.
- Mohan, R., Gogoi, S., Bora, A.J., Baruah, G., Bordoloi, S., Ali, A.A., Sarma, H.R., Dutta, R. K., 2020. Field experience of Fluoride Nilogon. *Curr. Sci.* 118 (2), 255–263. <https://doi.org/10.18520/cs/v118/i2/255-263>.
- Nath, S.K., Bordoloi, S., Dutta, R.K., 2011. Effect of acid on morphology of calcite during acid enhanced defluoridation. *J. Fluor. Chem.* 132 (1), 19–26. <https://doi.org/10.1016/j.jfluchem.2010.10.007>.
- Nath, S.K., Dutta, R.K., 2010. Fluoride removal from water using crushed limestone. *Indian J. Chem. Technol.* 17 (2), 120–125.
- Pan, S.Y., Haddad, A.Z., Gadgil, A.J., 2019. Toward greener and more sustainable manufacture of bauxite-derived adsorbents for water defluoridation. *ACS Sustain. Chem. Eng.* 7 (22), 18323–18331. <https://doi.org/10.1021/acssuschemeng.9b03649>.
- Rate, A.W., McGrath, G.S., 2022. Data for assessment of sediment, soil, and water quality at Ashfield flats reserve, Western Australia. *Data Brief.* 41, 107970. <https://doi.org/10.1016/j.dib.2022.107970>.
- Rathi, B.S., Kumar, P.S., Rangasamy, G., Badawi, M., Aminabhavi, T.M., 2024. Membrane-based removal of fluoride from groundwater. *Chem. Eng. J.* 488, 150880. <https://doi.org/10.1016/j.cej.2024.150880>.
- Reardon, E.J., Wang, Y., 2000. A limestone reactor for fluoride removal from wastewaters. *EST* 34 (15), 3247–3253. <https://doi.org/10.1021/es990542k>.
- Sdiri, A., Higashi, T., Jamoussi, F., Bouaziz, S., 2012. Effects of impurities on the removal of heavy metals by natural limestones in aqueous systems. *J. Environ. Manag.* 93 (1), 245–253. <https://doi.org/10.1016/j.jenvman.2011.08.002>.
- Shaji, E., Santosh, M., Sarath, K.V., Prakash, P., Deepchand, V., Divya, B.V., 2021. Arsenic contamination of groundwater: a global synopsis with focus on the Indian Peninsula. *Geosci. Front* 12 (3), 101079. <https://doi.org/10.1016/j.gsf.2020.08.015>.
- Shaji, E., Sarath, K.V., Santosh, M., Krishnaprasad, P.K., Arya, B.K., Babu, M.S., 2024. Fluoride contamination in groundwater: A global review of the status, processes, challenges, and remedial measures. *Geosci. Front* 15 (2), 101734. <https://doi.org/10.1016/j.gsf.2020.08.015>.
- Susheela, A.K. A treatise on fluorosis, Revised 2nd ed., Fluorosis Research and Rural Development Foundation, New Delhi, 2007.
- Turek, A., Wiczorek, K., Wolf, W.M., 2019. Digestion procedure and determination of heavy metals in sewage sludge— an analytical problem. *Sustain* 11 (6), 1753. <https://doi.org/10.3390/su11061753>.
- Turner, B.D., Binning, P., Stipp, S.L.S., 2005. Fluoride removal by calcite: evidence for fluorite precipitation and surface adsorption. *Environ. Sci. Technol.* 39 (24), 9561–9568. <https://doi.org/10.1021/es0505090>.
- UNICEF, (<https://www.unicef.org/yemen/water-sanitation-and-hygiene>), (2025).
- Varisco, D., 2019. Pumping Yemen dry: a history of Yemen's water crisis. *Hum. Ecol.* 47 (3), 317–329. <https://doi.org/10.1007/s10745-019-0070-y>.
- Weiss, M.I., 2015. A perfect storm: the causes and consequences of severe water scarcity, institutional breakdown and conflict in Yemen. *Water Int* 40 (2), 251–272. <https://doi.org/10.1080/02508060.2015.1004898>.
- WHO, 2017. Guidelines for Drinking-water Quality, Incorporating the First and Second Addenda. World Health Organization, Geneva.
- Xu, B., Liu, S., Zhou, J.L., Zheng, C., Weifeng, J., Chen, B., Zhang, T., Qiu, W., 2021. PFAS and their substitutes in groundwater: occurrence, transformation and remediation. *J. Hazard. Mater.* 412, 125159. <https://doi.org/10.1016/j.jhazmat.2021.125159>.
- Yemeni-Standards-for-Drinking-Water-Quality,2006, (https://www.researchgate.net/Fi/g/YemeniStandards-for-Drinking-Water-Quality_tbl1_226798069).